2

X-645-72-401

NASA TM X- 66083

NEUTRAL WINDS ABOVE 200Km AT HIGH LATITUDES

J. W. MERIWETHER
J. P. HEPPNER
J. D. STOLARIK
E. M. WESCOTT

OCTOBER 1972

GODDARD SPACE FLIGHT CENTER
GREENBELT, MARYLAND

Neutral Winds above 200 km at High Latitudes

by

J. W. Meriwether [1]
J. P. Heppner
J. D. Stolarik
E. M. Wescott [2]

October 1972

(1) Now at the High Altitude Laboratory, University of Michigan, Ann Arbor, Michigan, 48104

(2) Now at the Geophysical Institute, University of Alaska, College, Alaska

Abstract

Electrically neutral, luminous clouds are a by-product of chemical releases conducted to create barium ion clouds for the measurement of electric fields. Wind measurements provided by the motions of these clouds are particularly valuable in that the motions can be directly compared with convective, ion drift motions to test the importance of ion drag forces. Motion from multiple releases between 200 and 300 km from 15 rockets launched from 4 high latitude locations are analyzed in this paper. The observations in the evening and midnight hours at magnetic latitudes $\geq 65^{o}$ strongly suggest that in these regions ion drag is the dominant force in driving neutral winds between 200 and 300 km. This conclusion is based on both the agreement between ion and neutral drift directions, and the fact that there are distinct changes in the wind associated with (a) the reversal in east-west ion drift at the Harang discontinuity, and (b) the transition from auroral belt, sunward ion drift and polar cap, anti-solar ion drift. In the morning sector it is evident that neutral wind observations cannot be directly interpreted in terms of ion drag; other factors must be considered, such as inertial effects from ion drag, a lack of sufficient ionization for strong coupling of ion-neutral motions, and wind forces other than ion drag forces.

NEUTRAL WINDS ABOVE 200 KM AT HIGH LATITUDES

Introduction

A topic of ionospheric physics that is extremely important in the study of the dynamics of the upper atmosphere is the nature of the neutral winds at high latitudes for altitudes above 200 km. Theoretical global models (Geisler, 1966; Geisler, 1967; Kohl and King, 1967; King-Hele and Allan, 1966; Challinor, 1969; Challinor, 1970a) for the outer atmosphere have been constructed to delineate the broad details of the wind system and have been successful in explaining certain features of the F-region, (Duncan, 1969; Challinor, 1970b). The review article by Rishbeth (1972) provides considerable discussion on these topics. However, this approach, based upon the idea of day-to-night flow resulting from solar heating on the day side, does not take into account motions at high latitudes that are expected from the electric fields known to be present (see reviews by Maynard, 1972; Heppner, 1972c; Cauffman and Gurnett, 1972; Haerendel, 1971). Such neglect is serious because the plasma convection can generate neutral flow by ion drag and the resulting neutral winds may well be able to reverse the day-to-night flow.

Fedder and Banks (1972) discussed the consequences that can occur at high latitudes for a model that included the effects of convective flow and Joule heating. Their model considers the summer ionosphere at high latitudes where their results show a twin cell pattern in the neutral circulation. In the auroral belt, convective ion drift creates by ion drag a night-to-day neutral wind that dominates the day-to-night flow caused by solar heating. However, in the polar cap the neutral

wind created by ion convective flow supplements this day-to-night flow because the convective flow there is antisolar. The twin cell neutral pattern emerges as a result of using a two cell convection pattern for the plasma convection in the auroral belt. However, other considerations and the observations later discussed imply that modifications of this result are required.

For active magnetic periods, unusual effects can appear. Exceptionally high velocity neutral winds reaching speeds of 1000 m/s at high latitudes have been reported for the magnetic storm of May 26, 1967 from the accelerometer data of LOGACS (Feess, 1972; Bruce, 1972). On one occasion following storm activity in a series of TMA trail experiments from Hawaii, Smith (1968) found excessive speeds with values exceeding 200 m/s at altitudes near 140 km. Smith suggested that the flow direction to the southwest could be explained as a part of a cell system originating in high latitudes. Hays and Roble (1971) report two examples where the Doppler shift of λ6300 measured with a 15 cm interferometer corresponded to velocities of 300-400 m/s to the south for periods of considerable geomagnetic activity. Stoffregen (1972) in examining evening neutral winds measured with barium releases as a function of magnetic activity found that the neutral winds during active periods displayed enhanced speeds and directional shifts relative to the winds found for quiet periods; explanation was sought in terms of nightside heating and temperature gradients in the auroral zone. Rees (1970) found a correlation between the velocity of the east-west winds at an altitude of 160 km and the north-south magnetic disturbance averaged for the period of two hours prior to the occurrence of a negative bay. All these measurements show conclusively that knowledge of neutral winds cannot be predicted

on the basis of a single physical phenomenon such as solar heating, especially for periods of active magnetic disturbances. Thus, the complexity of the problem suggests a need for extensive data to obtain a reasonable picture of the physical processes present.

Direct access to the flow pattern of ionic and neutral constituents of the ionosphere at high altitudes is offered by the technique of barium releases from sounding rockets using such small amounts that the material released acts as a tracer agent and does not significantly perturb the dynamics of the interactions between the neutral and ionic components of the atmosphere. For release altitudes above 180 km, where the ratio between the ion gyrofrequency and the collision frequency is much greater than 1, and for cannister weights of 2-3 kg, this condition is believed to exist (Haerendel et al., 1967; Wescott et al., 1969). Direct comparison of the ion track with the neutral track during the period of observations makes possible an evaluation of the ion drag force. At these high release altitudes, there should not be any confusion regarding the direction of this force since the barium ions respond to the $\underset{\sim}{E} \times \underset{\sim}{B}$ drift; Fedder and Banks (1972), for example, have shown that rotation of the wind vector as a result of viscosity and collisions generally becomes important only below 200 km.

Data Acquisition

As a part of a continuing program of high latitude barium cloud releases, an accumulation of data concerning the direction and magnitude of neutral winds has been obtained. The program, conducted by the Goddard Space Flight Center (Wescott et al., 1969; Wescott et al., 1970;

Heppner et al., 1971), has in the past been primarily devoted to the measurement of electric fields from analysis of motions of the ion clouds. The large number of rocket flights and releases now make it possible to examine the neutral wind data in terms of geomagnetic and geographic coordinates, and convection patterns for the ion drag. The releases permit the acquisition of a crude height profile of the neutral winds between 200 and 300 km. More recently from Hall Beach, Canada (March 1971) and College, Alaska (March 1972) the profile has been extended downward to 85 km with the addition of a TMA/TEA trail release on the downleg of the rocket trajectory. Excluding these flights with TMA/TEA trails, for which the data reduction has not been completed, there have been 15 flights at high latitudes with most of the releases above 200 km. Four releases are conducted with each rocket with nominal release altitudes at 230 km and 300 km on both the ascent and descent legs of the trajectory. The latitudinal distribution of the releases covers about one degree with the trajectory of the rocket normally along a geomagnetic meridian. Details relating to the payload and camera stations can be found in Wescott et al., (1969) and Heppner et al., (1971).

Launching Sites

The locations of the releases may be divided into three regions - auroral belt, polar cap and at the transition between the auroral belt and the polar cap. The auroral belt measurements include launches from Norway in September of 1967 and 1968 and from Poker Flats, Alaska, in March 1970, the polar cap releases were carried out from the DEWLine site (Pin-Main) at Cape Parry, Canada, in March 1969, and the transition zone measurements from the DEWLine site (Bar-Main) at Barter Island, Alaska,

in March 1970. The flights from Poker Flats and Barter Island include two pairs of simultaneous launches: during evening twilight on March 2, 1970 and during morning twilight on March 4, 1970. It is convenient to use the terms "auroral belt" and "polar cap" to distinguish between areas of convective flow, respectively, toward the sun and away from the sun (i.e., solar and anti-solar flow). The purpose for making this distinction is that if one examines the geographical latitudinal distribution of the flights (66^{o}-72^{o}) it is not obvious on the basis of geography alone that there may be two groups of flights with different behaviorial characteristics. However, the geomagnetic coordinate system makes the division into two groups more readily discernable thereby creating a need for a label for each group. With this distinction the body of data includes nine auroral belt flights, three polar cap flights, and three transition zone flights. This latter term describes a situation where the behavior of a set of ion clouds reflects both the features of the auroral belt and the polar cap during the course of observations.

Data Reduction

The description of the data reduction procedure found in Wescott et al., (1969) and Heppner et al., (1971) for the derivation of the ion cloud tracks with triangulation from three camera stations explains the procedure used to analyze the neutral cloud motions. Although for neutral clouds the analysis is simpler because striations are not present, the interval for which data can be obtained is considerably less because the neutral clouds expand and spherically disperse by diffusion. Thus soon after the initial release it becomes difficult to assign an accurate center for a particular cloud in a photograph. This problem is most

restrictive for the clouds released near 300 km where diffusion is much more rapid than for those released near 200 km. Generally, the data for the higher clouds may be reduced for a period of 3 to 5 minutes and for the lower clouds from ten to fifteen minutes.

With a sequence of three photographs per minute, not many positional points are available to define a track. Because practically all the tracks examined indicated no change in direction of motion during the observing period, the measurements were averaged to obtain an average velocity vector for a particular cloud. Similarly, the positional information was averaged to produce an average height and average geographical coordinates for the location of each cloud. The values found with this procedure are the ones used in the figures presented. The errors in direction and speed from examination of the range of values of the individual data points are estimated to be about $\pm$ 10° and 20 m/s for the lower clouds and $\pm$ 20° and 40 m/s for the higher clouds. The data originating from the later flights are better in quality because refinements in the data reduction process led to more accurate positional information.

It was not possible to obtain data for all of the releases that occurred. The high clouds disperse so rapidly that if one or two minutes of data during the initial period of release are lost, as a result of obscuration by another neutral cloud or as a result of inadequate photographic coverage, it becomes difficult to establish an accurate track from the remaining data for that cloud. In this paper the release is omitted if the data for a track covers a time period of less than three minutes unless the quality of the data for the few points measured justify retention.

Data Presentation

Figures 1 and 2 present the ion and neutral velocities for the six evening auroral belt launches from Norway together with geographical coordinates and invariant latitudes, Λ , to define the location of each velocity vector. The display of information concerning the ion cloud motions in these figures, as well as the others below, is intended to present only a crude representation. More accurate tracks can be found in Wescott et al. (1969), Wescott et al. (1970), and Heppner et al. (1971). Figure 3 shows the data for the polar cap flights of March 1969, from Cape Parry, NWT, Canada, including one morning and two evening launches. Figure 4 shows the neutral wind velocities found in one evening and two morning flights from Barter Island, Alaska. The ion cloud motions were complex suggesting a response to both auroral belt and polar cap fields as a function of time and location. Figures 5 and 6 present the neutral wind motions for the two sets of simultaneous launches from Barter Island and Poker Flats, Alaska, together with a representation of the auroral forms present for each launch. For the other morning launch from Poker Flats (March 3, 1970) results very similar to that of the morning simultaneous launch (March 4, 1970) were found so a graphical presentation is omitted. Greenwich universal time is given for all dates.

1. Evening auroral belt flights from Norway

The analysis here pertains to Figures 1 and 2 which present the data for the neutral wind motions for the six Norway flights. The ion cloud motions for the August 31, 1967 and September 2, 1967 flights were eastward in conjunction with negative bays in the H component at Andøya, Kiruna, and Tromsø. In both cases the barium releases came

during the initial phase of a negative bay (magnetograms are in Wescott et al., 1969) and after a substantial positive bay deflection. The neutral wind for the August 31 flight was to the southeast for the high releases and south for the low releases. The September 2 flight provided similar results for the first pair of low and high releases, but the fourth cloud was released at 175 km (i.e., lower than planned) and the wind showed the interesting result of a southwest flow.

Three flights, September 12, 1967, September 20, 1968, and September 21, 1968, took place from Andøya, Norway, at a time of positive bay activity in the H component at Tromsø and Andøya. In each of these flights, the initial convective flow indicated by the ion clouds was essentially westward, but the complete analyses show a more complicated behavior with time related to the auroral breakup transitions (Wescott et al., 1969; Wescott et al., 1970). Only the first release of the September 12, 1967 flight provided suitable data on the neutral winds; the direction and magnitude of this wind was similar to the first releases of the two earlier flights, i.e., a drift to the south of 200 m/s. In the other two flights (see Figure 2) the neutral wind for all the releases was very similar in direction to the motion of the ions with speeds which were 20 to 50 percent of the ion speeds.

The last evening flight from Norway, September 23, 1968, occurred during a magnetically quiet period, and no systematic drift to either the east or west was observed for the ion clouds. Electric fields were of low magnitude (less than 10 mV/m) and extremely variable in direction. The neutral winds had a strong component to geomagnetic north unlike the previous flights which indicated a component to the south.

2. Polar cap flights

The polar cap flights were launched during twilight from Cape Parry, NWT, Canada, on the morning of March 7 and the evenings of March 8 and 9, 1969. In all three flights auroral activity was present considerably southwards of the releases (see Heppner et al., 1971). As shown in Figure 3 the ion clouds for the morning and evening releases moved westward and eastward respectively. The motions of the neutral clouds for the two evening flights are almost identical with a direction to the northeast. In contrast, the neutral clouds for the morning flight moved to the southwest, but the release at 278 km was more westward than the two lower releases. Three releases, cloud 1 of the March 8, 1969 flight and clouds 1 and 2 of the March 9, 1969 flight, persisted for such a period that a shift in the velocity direction was observed as the clouds fell. Representation of this effect is presented by two vectors, each showing the motion averaged over a period of about five minutes.

In all three flights, there appears to be no great difference in speed between the high releases and the low releases with values near 150 m/s being reasonably typical. However, the rocket for the last flight, March 9, 1969, was launched at a lower than nominal elevation angle so that the fourth cloud was released at 163 km, considerably below the nominal altitude. The neutral flow found from this release was 60 m/s, considerably less than the flow speed at higher altitudes.

3. Flights from central and northern Alaska in March 1970

The flights from Barter Island, Alaska, were planned as a part of a sequence of simultaneous pairs of flights from both Barter Island and Poker Flats, Alaska, but weather and technical problems permitted

only two twin launches: during the evening on March 2, 1970, and during the morning on March 4, 1970. Individual launches were conducted on March 3, 1970 (morning) from Poker Flats and on March 5, 1970 (morning) from Barter Island. Figure 4 shows the motions of neutral clouds for the flights from Barter Island. Figures 5 and 6 present the neutral flow for clouds released in each simultaneous pair of flights; the auroral forms present for the initial period of the experiment are also shown. Liftoff times for the two rockets in the first twin launch were identical and in the second were separated by 12 minutes.

The motions of the ion clouds for each of the northern (i.e., Barter Island) flights were complicated and for simplicity have been omitted. During each flight directional changes exceeding 90^{o} were observed: for flight 18.87 the assemblage of ion tracks resembles one large loop, during flight 18.88 each ion cloud completed a small loop over a short period of time within the total observing period, during flight 18.89 both spatial reversals and large changes in direction as a function of time were observed. The review by Heppner (1972c) includes a presentation of the ion tracks for flight 18.87. Basically, the motions appear to stem from responses to electric fields joining the auroral belt and polar cap regions (i.e., the continuity of convection between the two regions). This complexity was not observed in the neutral wind directions but the two northern morning flights of March 4 and March 5, 1970, showed very anomalous behavior in magnitudes. In one case (March 4) very high speeds for all four clouds were observed with 625 m/s being a typical value. In the other case (March 5) the velocities of the two highest clouds were two to three times greater

than the velocities of the two lowest clouds. A velocity gradient of this magnitude has not been observed in any other flight at comparable altitudes.

The behavior of the ion clouds for the southern launches was the normal response that has been found for auroral belt electric fields; i.e., the ion clouds of March 2, 1970 released prior to magnetic midnight moved westwards and the ion clouds of March 3 and March 4, 1970 released considerably after magnetic midnight moved eastwards. Figures 5 and 6 show the neutral cloud motions for the two sets of twin launches. The neutral flow found in the one individual southern launch on March 3 was very similar to that of March 4, namely a wind to the southwest with a speed of several hundred meters per second.

Data Summary

Velocity vectors for all data points have been collectively plotted in both geographic and geomagnetic coordinates. In both systems there are areas of coherence for the vectors from different flights but the geographical plots do not suggest any subsequent steps in analysis that might relate to cause. For example, in geographical local time and latitude regions where there is a lack of spatial coherence in the vectors it is not apparent that there are regional or local parameters unrelated to magnetic coordinates which could explain the variability. In turn, as noted below, fixed magnetic coordinates also restrict interpretation if the time-space variability of the convective pattern and associated auroral phenomena is not considered.

Figure 7 summarizes the data in geomagnetic coordinates in two altitude ranges. Major, or general, differences between data taken below

and above 240 km are not apparent but the vectors below 240 km tend to be slightly more variable than those above 240 km in some areas. In latitude-time sub-regions, such as near 17 and 23 hours MLT both above and below 240 km, the vector patterns suggest a spatial rotation of the wind. The additional analysis, below, illustrates that these rotations are centered along the boundary between the auroral belt and polar cap convection and the transition from westward to eastward convection near midnight.

Satellite and Ba^+ release experiments have both clearly shown that the gross pattern of high latitude electric fields, or convective flow, permits division into 3 regions: the polar cap, and the evening and morning auroral belts. The position of boundaries between these regions does, however, vary with activity conditions (i.e., time) and thus magnetic coordinates alone do not identify the region in which an observation was made. To locate the Figure 7 vectors relative to the convective regions a fixed representation for the location of boundaries was first constructed as shown in Figure 8. Inasmuch as more analytical modelling will be desirable in the future (and in response to various inquiries received, where an investigator wants to be able to mathematically represent the convective zones) considerable care was taken to make this representation as simple as possible without significantly deviating from statistically average boundary positions. Statistical positions for the polar cap-auroral belt boundary and the low latitude boundary for auroral belt convection were available from previous studies (Heppner et al., 1972b). It was found here that two circles with radii of 15° and 25°, respectively, gave a surprisingly good fit to these boundaries by locating their centers,

respectively, at 85° INV. lat. and 0000 MLT and 85° INV. lat. and 2230 MLT. An average position for the pre-midnight "Harang discontinuity," separating eastward and westward convective regions, was taken from a study of this discontinuity by Heppner (1972a). From OGO-6 measurements (Heppner, 1972b) it is known that the dayside equivalent of the Harang discontinuity is not a simple transition but instead a regional transition in which multiple complex electric field reversals are encountered. In Figure 8 this is only crudely represented by the step-like field reversals centered between 1000 and 1100 MLT.

To simplify the vector presentations in Figure 8, only one vector is shown per flight and this is either from the highest altitude release or the average of the two highest releases when they were at similar altitudes. Fourteen (14) of these fifteen (15) vectors are shown; the fifteenth case (Sept. 23, 1967) obviously does not fit into a pattern with others and the special conditions which accompanied it are discussed later. In locating the 14 vectors relative to boundary positions only a minimum amount of shifting relative to actual magnetic coordinates has been used. For example, all but one of the six vectors from Alaskan releases, and the morning vector from Pin-Main releases, are not shifted from their actual magnetic coordinate locations as these locations were already compatible with the measured convection and simultaneous location of auroral activity. The following steps were taken in shifting the other vectors. (1) The evening release from Bar-Main was shifted to a higher than actual latitude, but still within the auroral belt convection, to show its location adjacent to the polar cap boundary. (2) For the two evening Pin-Main vectors within the polar cap convection, the instantaneous polar cap-auroral belt

boundary location was not known so the northernmost simultaneous aurora was assumed to be at that boundary and the vectors were separated from the boundary by a latitudinal difference equal to one-half the instantaneous separation between the clouds and the northernmost aurora. (3) The vectors for Norway releases were shifted in magnetic local time, but not in latitude, to place them on the proper side of the Harang discontinuity as given by the simultaneous directions of ion cloud convection.

As illustrated by the result in Figure 8, the above steps bring about clear distinctions between polar cap and auroral belt winds in the evening hours and between winds preceding and following the Harang discontinuity. Thus, the necessity of knowing the instantaneous convection conditions to organize the data is demonstrated and this obviously implies that convective ion drag has a significant role in driving these winds.

This conclusion, last statement, is also indirectly supported by examination of the conditions accompanying the anomolous 15th vector (Sept. 23, 1967), noted previously, which was omitted from Figure 8. Figures 2 and 7 show a northward wind for this flight at a magnetic local time when either a westward or southward wind would be expected from the other flights. However, the simultaneous ion cloud motions and magnetic variations do not clearly indicate where this vector should be placed within a typical convection pattern. The simultaneous electric field was exceptionally weak and variable with both east and west motions superimposed on a variable north-south motion that had a long term tendency to be southward. The simultaneous magnetograms show that the flight took place during a quiet period about two hours after cessation of a period of storminess; for example, the 3-hour Kp index averaged about

4 for the preceding 24 hours, was 4+ for the 3-hour intervals 12-15 and 15-18 hours, but dropped to 1- for the 18-21 hour interval during which the flight took place. In total, because the instantaneous local ion drag force was extremely weak and variable a fit with other data on a convection plot cannot be evaluated. Although this explains a lack of fit, it does not explain cause for the northward wind with a magnitude almost as great as magnitudes typically observed. An explanation is not attempted here but two possibilities exist: either the anomolous behavior is related to a preceding change in the convection pattern and inertial effects are large, or, independent of ion drag there is a wind source approximately opposite to the global winds usually calculated for dayside heating.

Discussion

The extensive attempts in the past to theoretically model global wind systems illustrate that there are large uncertainties involved in estimating distributions and relative magnitudes for pressure gradient, ion drag, viscous, and inertial forces even when the space-time variability of atmospheric parameters is only partially recognized. The data here will not separate these variables but from the organization of vectors in Figure 8 it appears that one should be able to assess the conditions under which the ion drag force becomes dominant at high latitudes.

The drag on neutral constituents depends on ion and neutral densities, temperatures, and atmospheric composition as well as the electric field strength. An additional, and highly significant, factor in establishing a neutral wind system is the duration of ion flow in a particular direction. From the onset of ion drift in a given direction, there will

be a time delay before the bulk neutral flow induced by ion drag can reach its maximum speed. These factors are all altitude dependent. As shown by Fedder and Banks (1972), a comparison between the observed ion flow and neutral flow will not generally be valid except at reasonably high altitudes where viscosity and collision effects do not produce a significant rotation of the neutral wind vector. Their calculations illustrate that these effects drop off rapidly above 150 km and become relatively insignificant above 200 km; thus, the altitude range for most of the releases reported here should be ideal for revealing the influence of ion drag. Similarly, in the model given by Rishbeth (1972) the ion drag parameter has a broad maximum between 200 and 300 km.

The lack of major differences between winds above and below 240 km, noted previously, supports the calculations noted above. In finer detail, two flights shown in Figure 1 (August 31, 1967 and Sept. 2, 1967) indicate that the higher releases respond more quickly than the lower releases to a change in the ion flow. In these cases, in the early stages of a negative bay on the morning side of the Harang discontinuity, the direction of motion for the high neutral clouds is about 30^{o} closer to the direction of ion cloud motion than for the low neutral clouds. The relative rotation is consistent with a rotation of the ion flow from westward to southward to eastward in passing through the Harang discontinuity. The fact that there is still an angular difference, also of about 30^{o}, between the motions of the high neutral clouds and the direction of ion flow is also consistent with having a time delay between a change in the ion drag and the appearance of change in the neutral bulk motion. However, as noted later, the difference of roughly 30^{o}

between the ion cloud motions and the motions of the highest neutral clouds in these cases could also result from a vector addition of the local ion drag force and other forces.

As summarized in Figure 8, the wind directions observed in the evening auroral belt, westward convection, region agree well with expectations for an ion drag force. These releases occur when and where the convective ion flow has been sustained in one direction for several hours. In the polar cap and morning auroral belt regions of Figure 8 a similar close agreement is not found and it is obvious that other factors such as time duration and other wind forces must be considered. The number of possible variables suggests that each observation should be treated independent of others; however, a more comprehensive approach is suggested by both the relative coherence of the vectors and the fact that at this stage we are mainly seeking major effects.

If the numerous past models of global wind systems are reasonably realistic for the condition where there is not an ion drag driving force at high latitudes, one should be able to roughly approximate the total wind by vectorially adding an ion drag force to these models. In effect, however, our approach is one of seeing whether the vector properties of the global models are suitable for explaining deviations from the ion drag pattern. This veiwpoint, we believe, is justified on grounds that the pattern of convective ion drag is currently better known than the global distribution of temperatures and densities. The characteristics of a vector addition are illustrated in Figure 9, explained below.

Figure 9 (a) is a reproduction of the northern hemisphere global wind pattern given by Kohl and King (1967) for an altitude of 300 km, scale height of 60 km, and an electron density of 3×10^5 cm^{-3} (i.e, a high velocity wind condition giving an average value of 140 meters/sec). This model is chosen simply because it has been frequently referenced and reasonably represents the majority of such models. We have, for example, also used the recent models by Blum and Harris (1972) for vector additions like those in Figure 9 and found that differences in the result are insignificant relative to our objective, which is to find an explanation for deviations from the ion drag pattern.

The principal vector properties of the ion drag force, based on satellite electric field measurements and Ba^+ releases (Heppner, 1972(a), (b), and (c)), are shown in Figure 9(b). It is important to recognize that the force pattern will only completely describe the ion drag wind pattern when the collisional coupling between ions and neutrals is such that all inertial forces are zero or the flow is unidirectional for a long period of time. As the coupling is not perfect, or instantaneous, and the convection relatively abruptly changes direction in boundary regions, inertial effects must also be included.

In Figure 9(c) vectors representing the inertial wind from ion drag forces are drawn to illustrate the principal effects. These occur where the ion flow must abruptly change direction to maintain continuity. Examples are: (a) in the pre-noon sector of the auroral belt where multiple reversals of the electric field are observed the inertial effects will add complexity to the complex behavior already expected from space-time variations in the ion drag force, (b) at the transition from

polar cap to auroral belt flow on the nightside of the polar cap the inertia of the anti-solar polar cap wind will carry it into the auroral belt, as discussed further below, and (c) as a consequence of local time variations in the position of the auroral belt convective regions and the earth's rotation, inertia will carry the auroral belt wind into peripheral, lower latitude regions. This picture is greatly over simplified, particularly in that it ignores all gradients of the ion flow within each convective region. However, it illustrates that the inclusion of inertial effects is likely to be of primary importance in the nightside auroral belt, and further, that within the nightside auroral belt the effect will vary with magnetic local time. This night-time magnetic local time dependence should typically have the following characteristics. (1) In the post-twilight sector preceding the Harang discontinuity the effect on wind directions in the auroral belt will usually be small from both the standpoint of the duration of the inertial effect and the relative geometry. (2) In the vicinity of the Harang discontinuity the convection is observed, as shown in Figure 9(b), to have a large southward component which is interpreted to be a continuation of the polar cap flow extending to the southern boundary of the auroral belt convection. Thus at the Harang discontinuity inertial forces will drive a neutral wind southward into lower latitude regions. (3) From roughly midnight, near the Harang discontinuity, to approximately 0400 MLT the anti-solar polar cap convection turns eastward on entering the auroral belt. The inertia of the neutrals driven by this ion drag will cause them to penetrate more deeply into the auroral belt region. Thus, neutral constituents in at least the northern part of the auroral belt will be

subject to an anti-solar inertial force continuously for four or more hours. The depth of penetration into the auroral belt as a function of local time will depend on a number of factors which we cannot accurately estimate at this stage of analysis. Thus for illustration here we only assume that the average anti-solar inertial neutral wind will increase with local time as a consequence of the duration of the inertial force; numerical assumptions are given below.

In Figure 9, vector additions are shown as: (d) = (a) + (b), (e) = (b) + (c), and (f) = (a) + (b) + (c). Even though accuracy is not claimed in these representations, as their function is simply to illustrate effects, it is desirable to have internal consistency. For this purpose the following magnitudes were assumed. The winds at high latitudes in (a) were represented in magnetic coordinates by a velocity of 150 meters/sec directed toward 0130 MLT. For (b) ion velocities of 400 and 600 meters/sec were assumed, corresponding to electric fields of 24 and 36 volts/km, respectively, for the polar cap and auroral belt regions. The ion drag neutral wind was then assumed to have velocities equal to one-half the ion velocities (i.e., 200 and 300 meters/sec in polar cap and auroral belt regions, respectively). For magnitudes of the inertial wind on the nightside, a linear increase with magnetic local time was assumed beginning with 0 at 2100 MLT and reaching a maximum of 200 meters/sec (i.e., equal to the polar cap neutral wind) at 0300 MLT.

Comparison of the diagrams in Figure 9(d), (e), and (f) with the observation summary in Figure 8 brings out the following points. In the evening hours extending to the Harang discontinuity, the addition of winds

from global pressure gradients and inertial effects has very little effect on wind directions; thus the good agreement with ion drag forces remains. In the region near midnight, on the morning side of the Harang discontinuity, both the global wind and the inertial wind increase the southward component of the ion drag neutral wind and this appears to be supported by the observations, not only in terms of direction but also by a small increase in the magnitude. In the morning auroral belt, near 0300 MLT, both the global wind and the inertial wind rotate the ion drag neutral wind vector in the direction required to obtain agreement with the observations, but with the parameters used this rotation is not sufficient. In the polar cap only one of the five vectors in Figure 8 is in good directional agreement with an ion drag wind; the other four observed directions are rotated in the same sense expected from the addition of a global pressure gradient wind but the rotation is much too large to be explained by the global wind model of Figure 9(a).

From the above it is apparent that more accurate modelling is required to explain the auroral belt observations near 0300 MLT and most of the polar cap observations. Several reasonable possibilities exist. One is that we have underestimated inertial effects. For example, increasing the inertial wind could give agreement for the 0300 MLT auroral belt observations. Also for polar cap observations made close to the evening auroral belt boundary it is not unreasonable to speculate that the region of observation was previously within the auroral belt convection and that the observed wind is the resultant of this previously existing wind from auroral belt ion drag and the subsequent wind force from polar cap ion drag. This explanation could not, however, be applied

to the highest latitude polar cap observation in the early morning hours.

Another alternative is that ion densities in the nightside polar cap and early morning auroral belt may be less than at other times such that the ratio of ion to neutral densities is too small for the ion drag force to be effective. The observed wind would then more closely approximate the wind from global pressure gradients. The analysis of diurnal variations in total electron content by Liszka (1967) do indicate minimum densities near 0300 MLT at auroral latitudes. It does not, however, appear reasonable to expect a low ionization density at these altitudes for the polar cap cases near 1700 MLT.

A third alternative is that global wind models similar to that of Figure 9(a) are not representative of conditions that would exist in the absence of high latitude convection. For example, by properly adjusting magnitudes as a function of location a wind directed roughly from 1700 toward 0500 MLT would give a better fit to the polar observations. Relative to these observations the angle would be essentially the same in geographical coordinates.

Combinations of the above alternatives appear to be required if one is to explain each difference between the observed winds and the ion drag pattern. There are other possible effects which have been considered but they do not provide agreement with the data. For example, the Coriolis force on an anti-solar polar cap neutral wind would rotate the polar cap neutral wind in the opposite sense of the required rotation. Another example is nightside heating in the auroral belt which Stoffregen (1972) has proposed to explain winds observed in the evening hours from barium

releases conducted in Sweden. From our data the heating argument appears to be contrary to most of the observations except in the evening hours where it would produce winds in the same direction as ion drag. Abrupt changes at the Harang discontinuity and the morning hour flows toward the auroral activity from the adjacent polar cap appear to contradict the heating mechanism. Even for the case of the anomolous 15th vector, discussed under "Data Summary," explanation in terms of heating does not appear promising unless one could demonstrate that the region south of the observations remained hot for periods exceeding several hours following the disturbance.

In summary, the most typical observations in the evening and midnight hours can be modelled in terms of ion drag forces with only minor allowances for inertial effects. However, in the morning hours it appears likely that an additional wind force is required even when inertial effects from ion drag are assumed to be large. Pressure gradients from auroral belt heating do not appear to be a likely source for this additional force; pressure gradients from global heating patterns could be important but a distribution different than that of past models is required. The data acquired from releases subsequent to those reported here, and data recently acquired in Alaska by the interferometer technique described by Hays and Roble (1967) should aid in future attempts to separate the many variables that conceivably influence the neutral wind.

Acknowledgments

We are particularly grateful to Mrs. Mary Miller for her excellent work in reducing photographic plates and performing triangulation calculations. One of us (JWM) wishes to thank the National Academy of Sciences for the support provided under a postdoctoral associateship during the performance of this research and the University of Michigan for support provided under NSF Grant GA-28690X2 during the final preparation of this paper.

References

Blum, P. W. and I. Harris, The global wind system in the thermosphere; preprint of paper presented at COSPAR, Madrid, Spain (to appear in Space Research XIII) 1972.

Bruce, R. W., Upper atmosphere density determined from Logacs, Space Res., 12 (in press) 1972.

Cauffman, D. P. and D. A. Gurnett, Satellite measurements of high latitude convection electric fields, Space Sci. Rev., 13, 369-410, 1972.

Challinor, R. A., Neutral-air winds in the ionospheric F-region for an asymmetric global pressure system, Planet. Space Sci., 17, 1097-1106, 1969.

Challinor, R. A., Neutral-air winds in the ionospheric F-region for an asymmetric global pressure system, Planet. Space Sci., 20, 1485-1488, 1970a.

Challinor, R. A., The behavior of the Arctic F-region in winter, J. Atmos. Terr. Phys., 32, 1959, 1970b.

Duncan, R. A., Neutral winds and universal time control of the polar F-region, J. Atmos. Terr. Phys., 31, 1008-1009, 1969.

Freess, W. A., Upper atmospheric winds determined from the Logacs experiment, Space Res., 12 (in press) 1972.

Fedder, J. A. and P. M. Banks, Convection electric fields and polar thermospheric winds, J. Geophys. Res., 77, 2328-2340, 1972.

Giesler, J. E., Atmospheric winds in the middle latitude F region, J. Atmos. Terr. Phys., 28, 703-720, 1966.

Giesler, J. E., A numerical study of the wind system in the middle thermosphere, J. Atmos. Terr. Phys., 29, 1469-1482, 1967.

Hays, P. B., and R. G. Roble, Direct observations of thermospheric winds during geomagnetic storms, J. Geophys. Res., 76, 5316-5321, 1967.

Haerendel, G., Plasma drifts in the auroral ionosphere derived from barium releases, preprint of paper presented at the meeting, "Earth's Particles and Fields", Cortina, Italy, Sept. 1971.

Haerendel, G. R., R. Lüst, and E. Rieger, Motion of artificial ion clouds in the upper atmosphere, Planet. Space Sci., 15, 1-18, 1967.

Heppner, J. P., J. D. Stolarik, and E. M. Wescott, Electric-field measurements and the identification of currents causing magnetic disturbances in the polar cap, J. Geophys. Res., 76, 6028-6053, 1971.

Heppner, J. P., The Harang discontinuity in auroral belt ionospheric currents, Geofys. Publ., Special Edition, Minneskift for Prof. L. Harang (ed. by J. Holtet and A. Egeland) 29, 105-120, 1972a,

Heppner, J. P., Electric field variations during substorms, Planet. Space Sci., 20 (in press) 1972b.

Heppner, J. P., Electric fields in the magnetosphere, Proc. of the Symposium on Critical Problems of Magnetospheric Physics, Madrid, Spain, May 1972 (in press) 1972c.

King-Hele, D. G. and R. R. Allan, The rotational speed of the upper atmosphere, Space Sci. Rev. 6, 248-272, 1966.

Kohl, H. and J. W. King, Atmospheric winds between 100 and 700 km and their effects on the ionosphere, J. Atmos. Terr. Phys., 29, 1045-1062, 1967.

Liszka, L., The high latitude trough in ionospheric electron content, J. Atmos. Terr. Phys., 29, 1243-1259, 1967.

Maynard, N. C., Electric fields in the ionosphere and magnetosphere, Magnetosphere-Ionosphere Interaction, (ed. by K. Folkestad) Universitetsforlaget, Oslo; 155-168, 1972.

Rees, D., Ionospheric winds in the auroral zone, J. Brit. Inter. Soc. 24, 233-246, 1971.

Rishbeth, H., Thermospheric winds and the F-region: a review, J. Atmos. Terr. Phys., 34, 1-48, 1972.

Smith, L. B., An observation of strong thermospheric winds during a geomagnetic storm. J. Geophys. Res., 73, 4959-4963, 1968.

Stoffregen, W., The anomaly of the neutral wind at a height of $\simeq$ 200 km at high latitudes, Magnetosphere-Ionosphere Interactions, (ed. by K. Folkestad) Universitetsforlaget, Oslo; 83-86, 1972.

Wescott, E. M., Stolarik, J. D., and Heppner, J. P., Electric fields in the vicinity of auroral forms from motions of barium vapor releases, J. Geophys. Res., 74, 3469-3487, 1969.

Wescott, E. M., Stolarik, J. D., and Heppner, J. P., Auroral and polar cap electric fields from barium releases, Particles and Fields in the Magnetosphere (ed. by B. M. McCormac) D. Riedel Publ. Co., Dordrecht, 229, 1970.

Figure Captions

Figure 1: Neutral wind vectors (N) for three flights from Andennes, Norway in 1967. Gross motions of the ion clouds (I) are also shown. R1, R2, R3, and R4 are the release points.

Figure 2: Neutral wind vectors for three flights from Andennes, Norway in September 1968. Ion motions not shown in the case of rocket 18.77 were slow and highly irregular (see text).

Figure 3: Neutral wind vectors for one morning (18.83) and two evening (18.84, 18.85) flights from Cape Parry, NWT, Canada in March 1969.

Figure 4: Neutral wind vectors for one evening (18.87) and two morning (18.88, 18.89) flights from Barter Island, Alaska in March 1970. Ion motions for all flights were complex (see text).

Figure 5: Neutral wind vectors for simultaneous evening flights from Barter Island (Bar-M) and Poker Flats, Alaska. Lift-offs occurred at 0430 UT at both sites. Locations of auroral forms at 0436:40 UT are shown at a projected height of 120 km.

Figure 6: Neutral wind vectors for morning flights from Barter Island and Poker Flats, Alaska on March 4, 1970. Lift-off times were 1430 UT and 1442 UT, respectively. Locations of auroral forms at 1445 UT are shown at a projected height of 120 km.

Figure 7: Neutral wind vectors in geomagnetic coordinates.

Figure 8: Neutral wind vectors summarized relative to a fixed representation of the three convection regions: polar cap, evening auroral belt, and morning auroral belt. One vector per flight for 14 flights. See text for 15th flight.

Figure 9: Illustrative representation of the: (a) northern hemisphere global wind given by Kohland King (1967); (b) high latitude distribution of the convective ion drag force, or the neutral wind driven by ion drag for perfect coupling and zero inertia; (c) inertial wind from ion drag forces; (d) vector addition of (a) and (b); (e) vector addition of (b) and (c); and (f) vector addition of (a), (b) and (c).

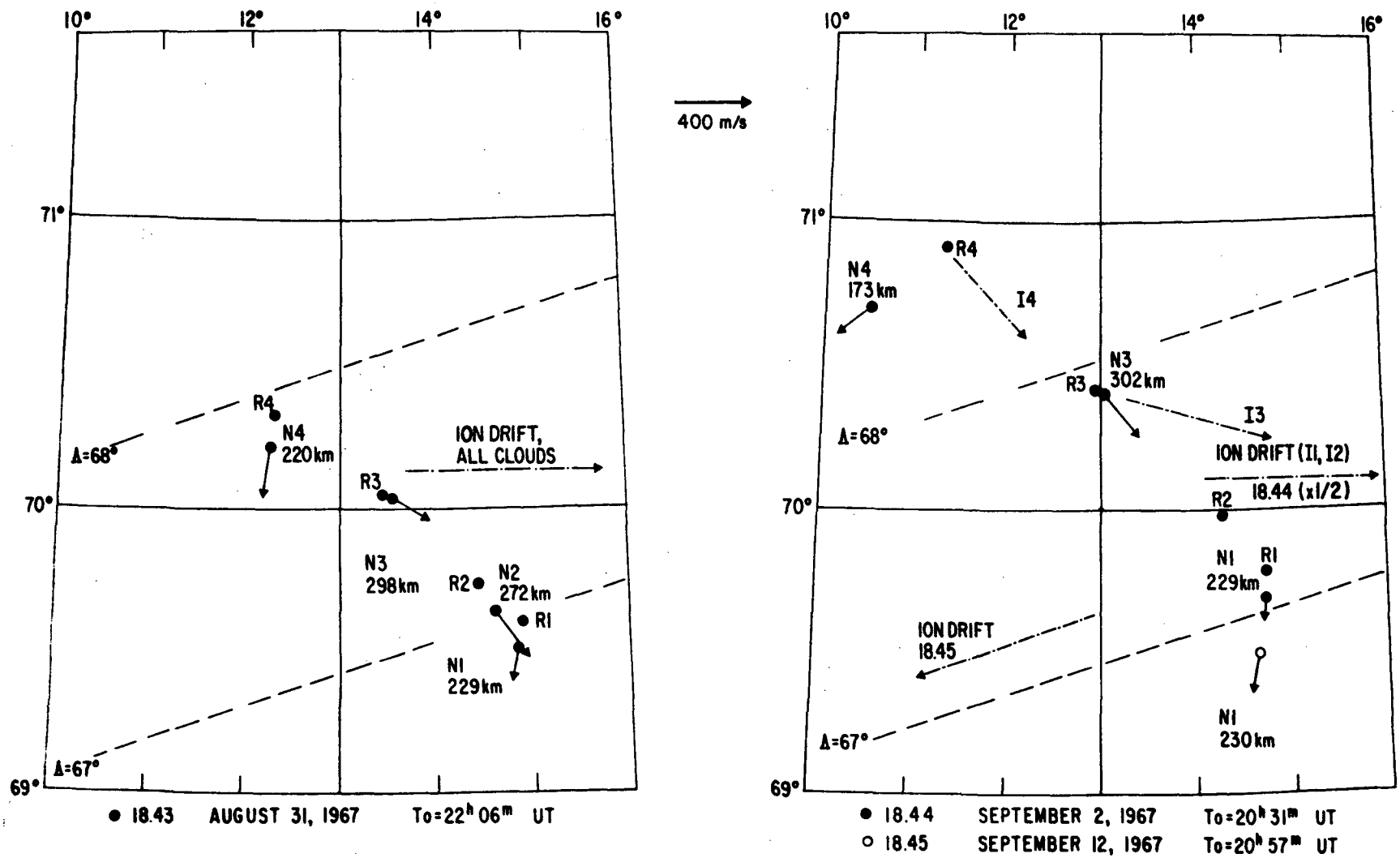
10°
12°
14°
16°
71°
70°
69°
400 m/s
R4
N4
220km
A=68°
ION DRIFT,
ALL CLOUDS
R3
N3
298km
R2
N2
272km
R1
N1
229km
A=67°
● 18.43 AUGUST 31, 1967 To=22h 06m UT
N4
173km
I4
N3
302km
I3
ION DRIFT (I1, I2)
18.44 (x1/2)
ION DRIFT
18.45
N1
230km
● 18.44 SEPTEMBER 2, 1967 To=20h 31m UT
○ 18.45 SEPTEMBER 12, 1967 To=20h 57m UT

Figure 1

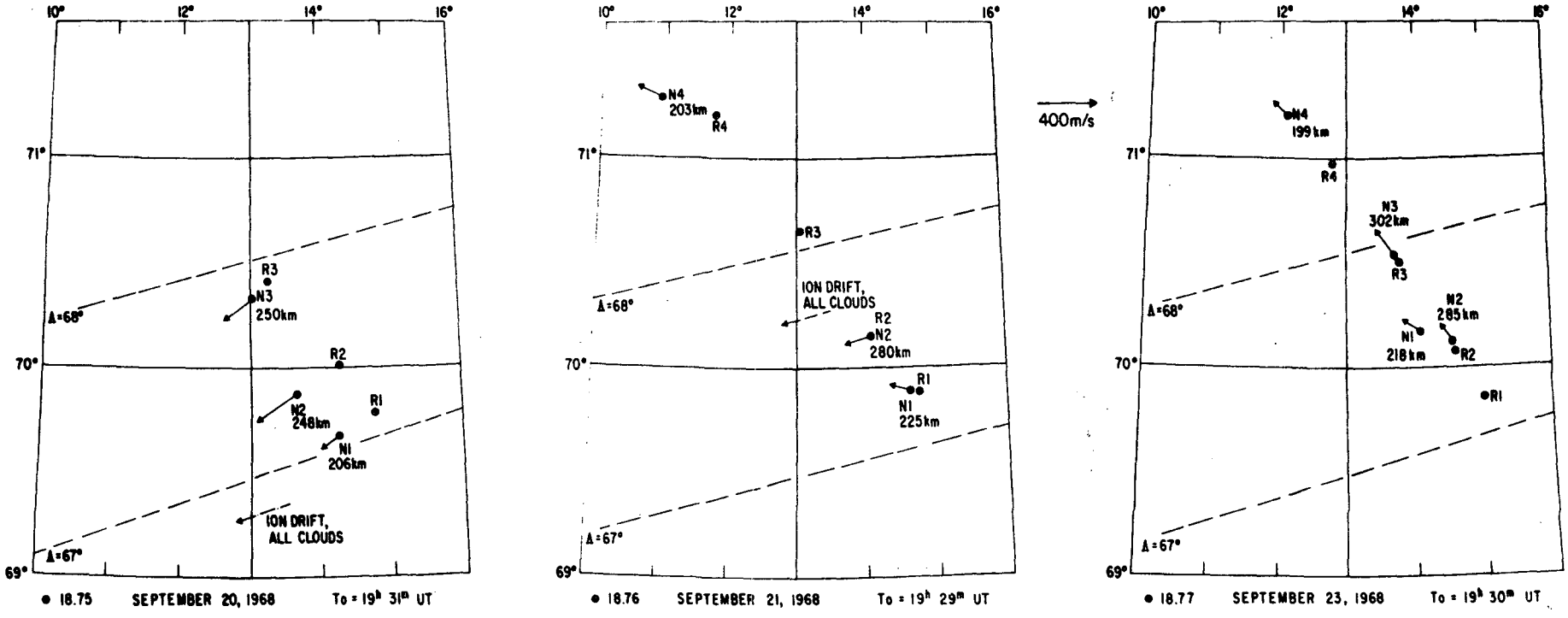
10°
12°
14°
16°
71°
70°
69°
A=68°
A=67°
R3
N3
250km
R2
N2
248km
R1
N1
206km
ION DRIFT,
ALL CLOUDS
• 18.75 SEPTEMBER 20, 1968 To = 19h 31m UT
N4
203km
R4
ION DRIFT,
ALL CLOUDS
R2
N2
280km
R1
N1
225km
• 18.76 SEPTEMBER 21, 1968 To = 19h 29m UT
400m/s
N4
199km
R4
N3
302km
R3
N2
285km
N1
218km
R2
R1
• 18.77 SEPTEMBER 23, 1968 To = 19h 30m UT

Figure 2

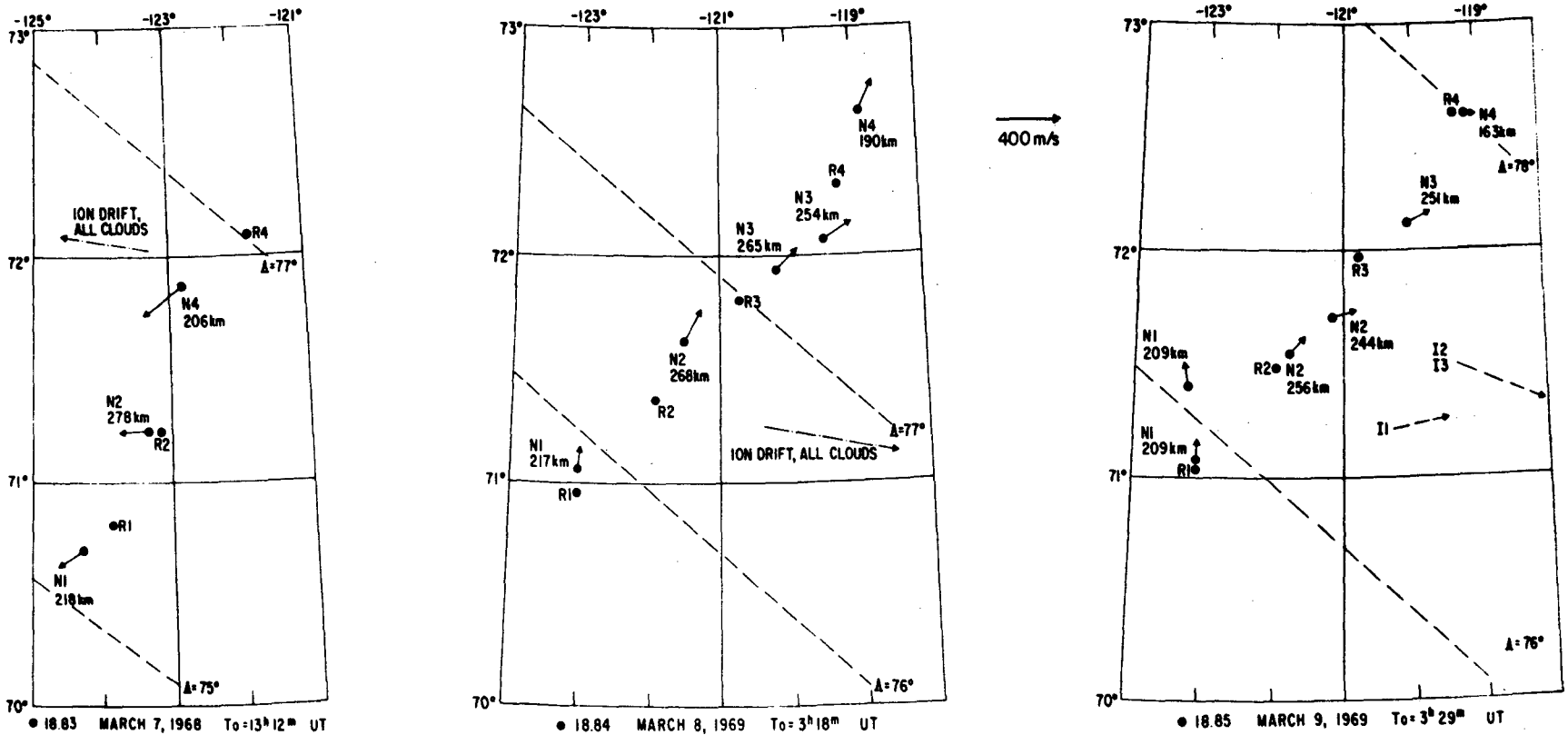
-125°
-123°
-121°
73°
72°
71°
70°
ION DRIFT, ALL CLOUDS
R4
A=77°
N4
206km
N2
278km
R2
R1
NI
218km
A=75°
● 18.83 MARCH 7, 1968 To=13h12m UT
-123°
-121°
-119°
N4
190km
R4
N3
254km
N3
265km
R3
N2
268km
R2
A=77°
NI
217km
ION DRIFT, ALL CLOUDS
RI
A=76°
● 18.84 MARCH 8, 1969 To=3h18m UT
400 m/s
-123°
-121°
-119°
R4
N4
163km
A=78°
N3
251km
R3
N2
244km
NI
209km
R2
N2
256km
I2
I3
I1
NI
209km
RI
A=76°
● 18.85 MARCH 9, 1969 To=3h29m UT

Figure 3

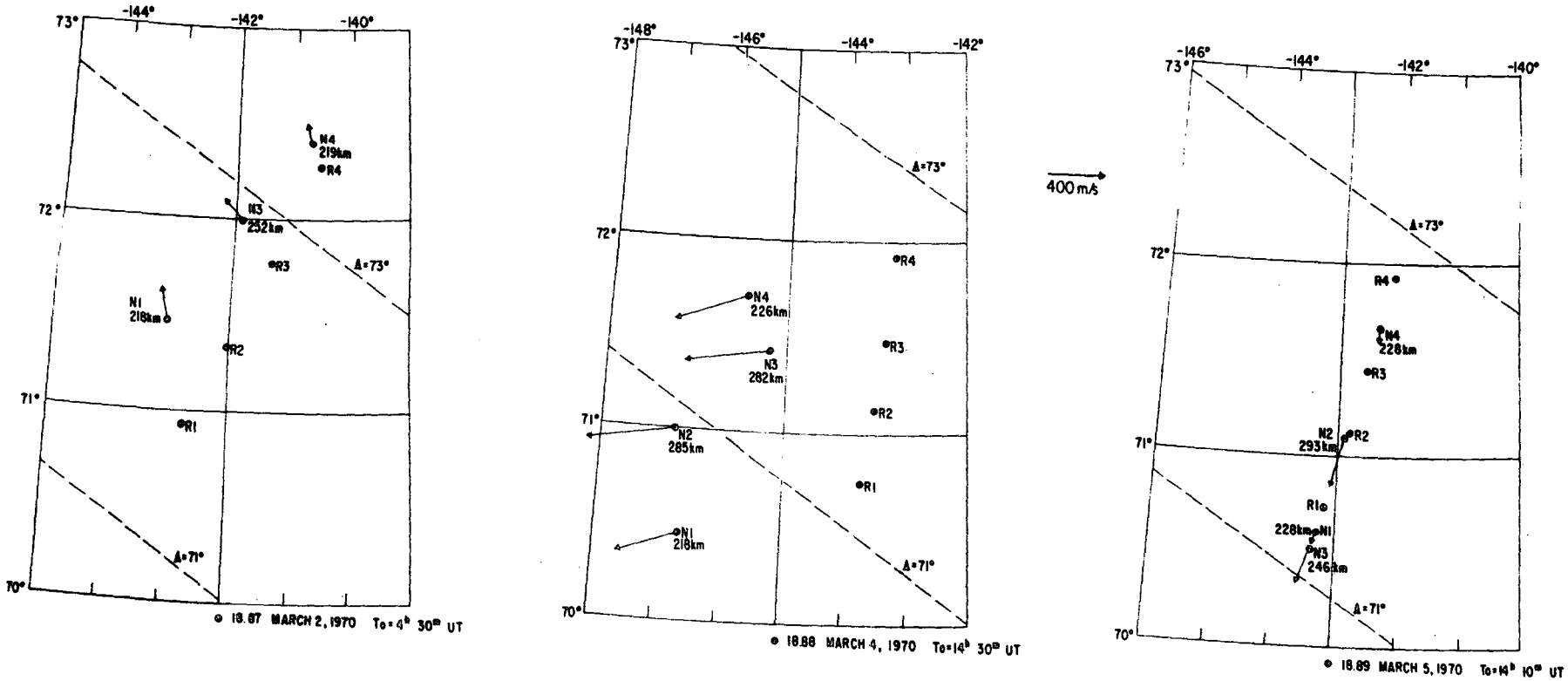
73°
-144°
-142°
-140°
72°
71°
70°
N4
219km
R4
N3
252km
R3
Δ=73°
N1
218km
R2
R1
Δ=71°
18.87 MARCH 2, 1970 To=4h 30m UT
-148°
-146°
-144°
-142°
Δ=73°
N4
226km
R4
N3
282km
R3
N2
285km
R2
R1
N1
218km
Δ=71°
18.88 MARCH 4, 1970 To=14h 30m UT
400 m/s
-146°
-144°
-142°
-140°
Δ=73°
R4
N4
228km
R3
N2
293km
R2
R1
228km
N1
N3
246km
Δ=71°
18.89 MARCH 5, 1970 To=14h 10m UT

Figure 4

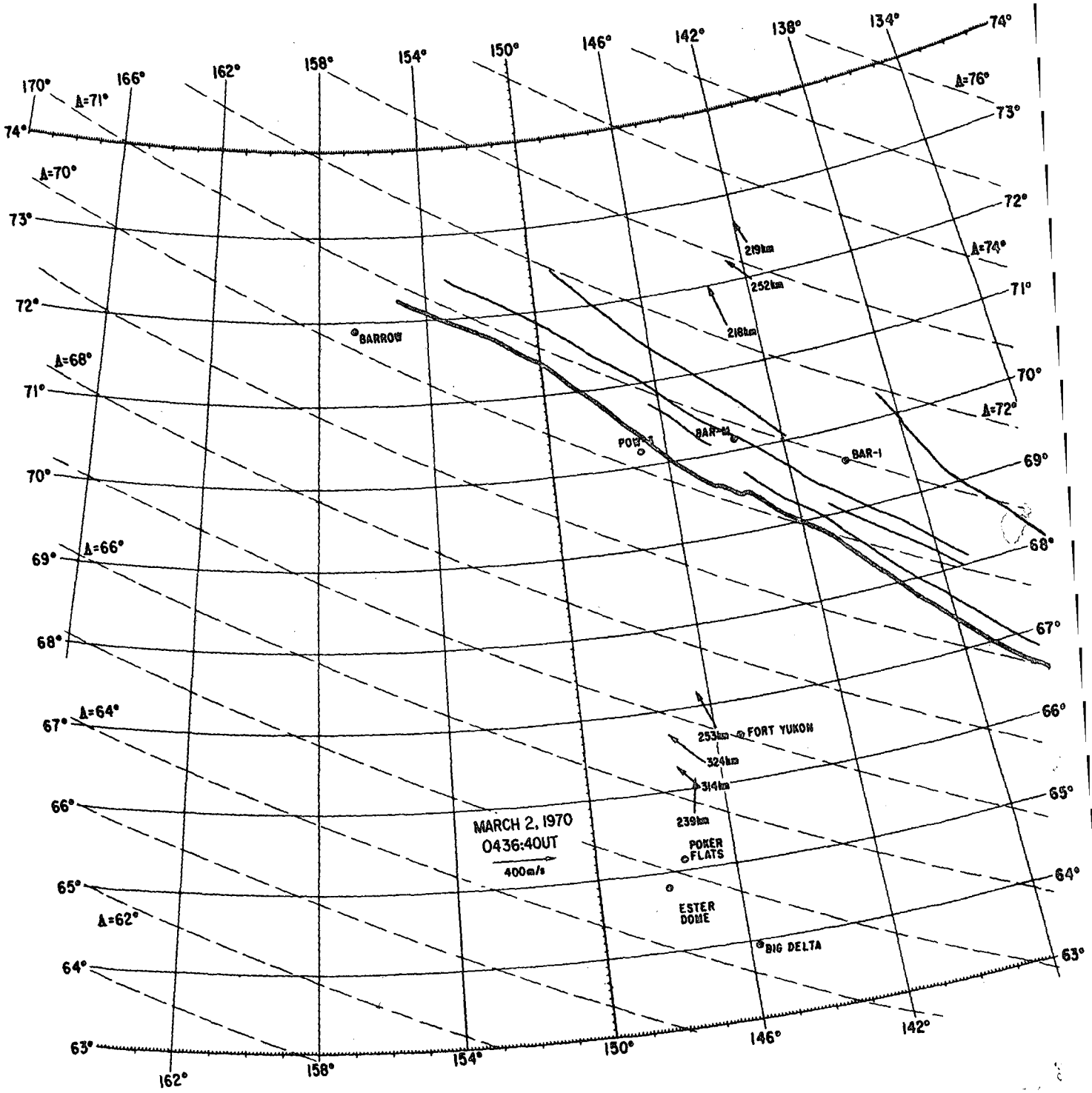
MARCH 2, 1970
0436:40UT
400m/s
BARROW
POKER FLATS
ESTER DOME
FORT YUKON
BIG DELTA
BAR-1
219km
252km
218km
253km
324km
314km
239km
A=76°
A=74°
A=72°
A=70°
A=68°
A=66°
A=64°
A=62°
A=71°

Figure 5

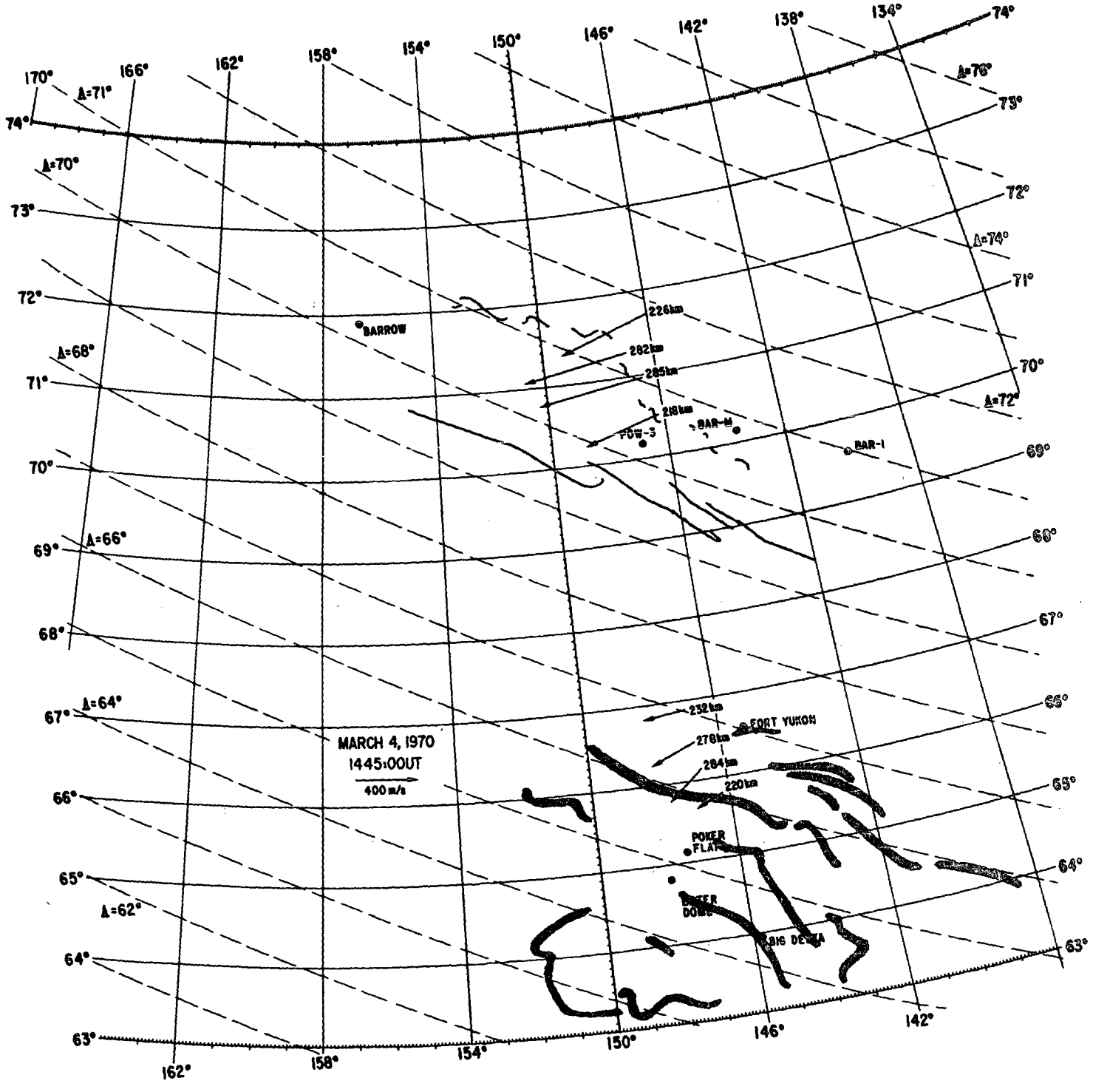
MARCH 4, 1970
1445:00UT
400 m/s
BARROW
POW-3
BAR-M
BAR-I
FORT YUKON
POKER FLAT
226km
282km
285km
218km
232km
278km
284km
220km
A=71°
A=70°
A=68°
A=66°
A=64°
A=62°
A=76°
A=74°
A=72°

Figure 6

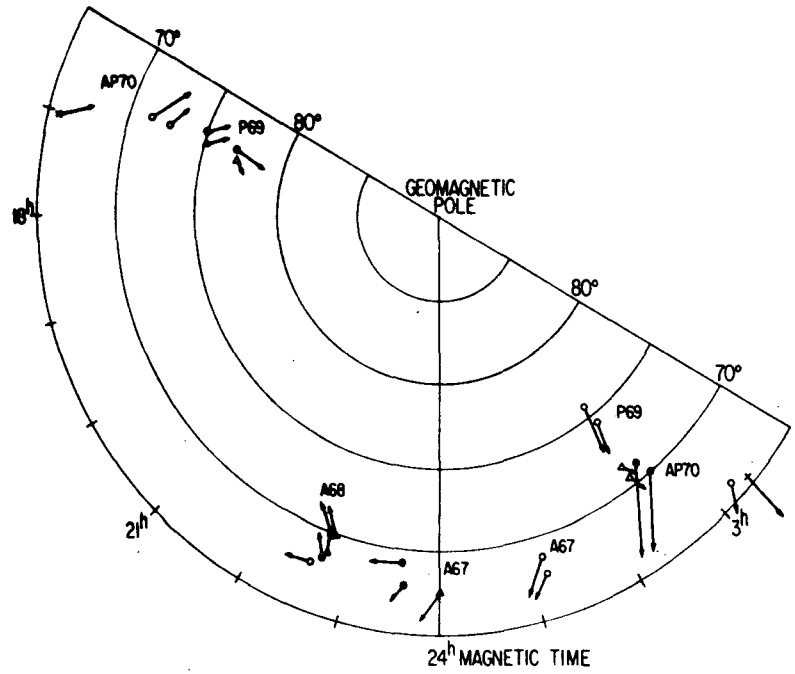

BARIUM RELEASES BELOW 240 Km

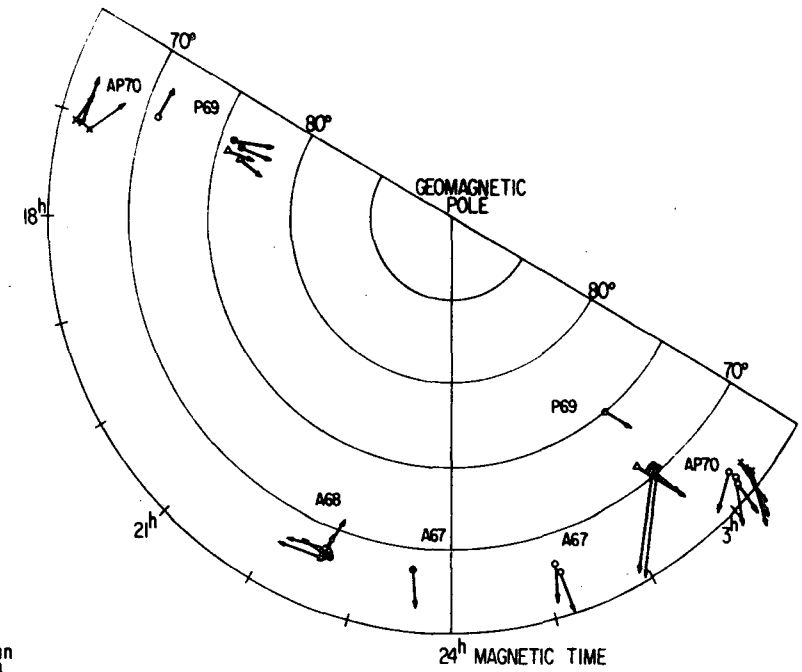

BARIUM RELEASES ABOVE 240 Km

Sun

400 m/s

EVENING LAUNCHES

A67 ANDENES, NORWAY – 1967
- ∘ 18.43
- • 18.44
- △ 18.45

A68 ANDENES, NORWAY – 1968
- ∘ 18.75
- • 18.76
- △ 18.77

P69 CAPE PARRY, CANADA – 1969
- • 18.84
- △ 18.85

AP70 BARTER ISLAND, ALASKA – 1970
- ∘ 18.87

POKER FLATS, ALASKA – 1970
- × 18.90

MORNING LAUNCHES

P69 CAPE PARRY, CANADA – 1969
- ∘ 18.83

AP70 BARTER ISLAND, ALASKA – 1970
- • 18.88
- △ 18.89

POKER FLATS, ALASKA – 1970
- × 18.108
- ∘ 18.109

Figure 7

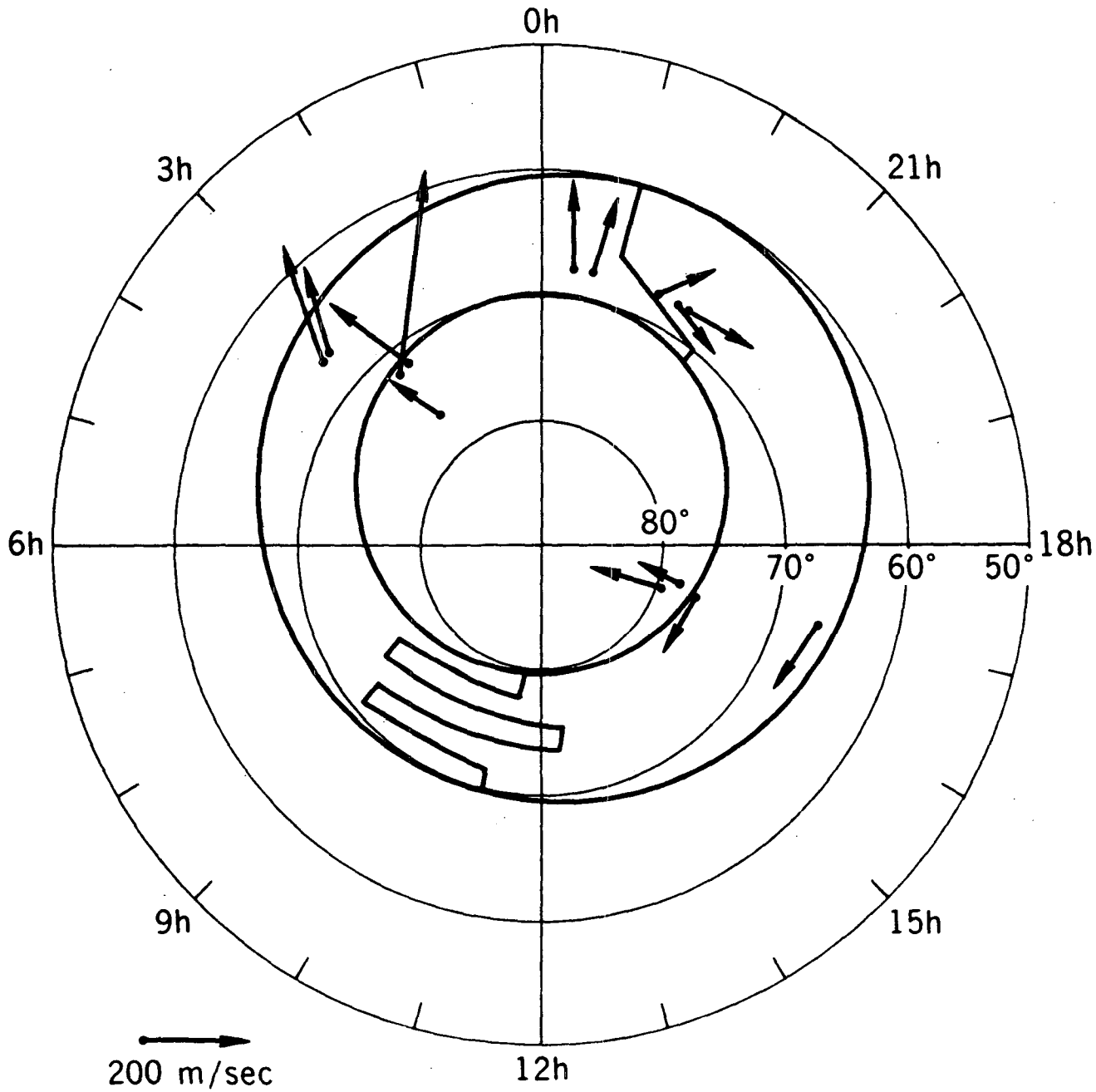

Figure 8

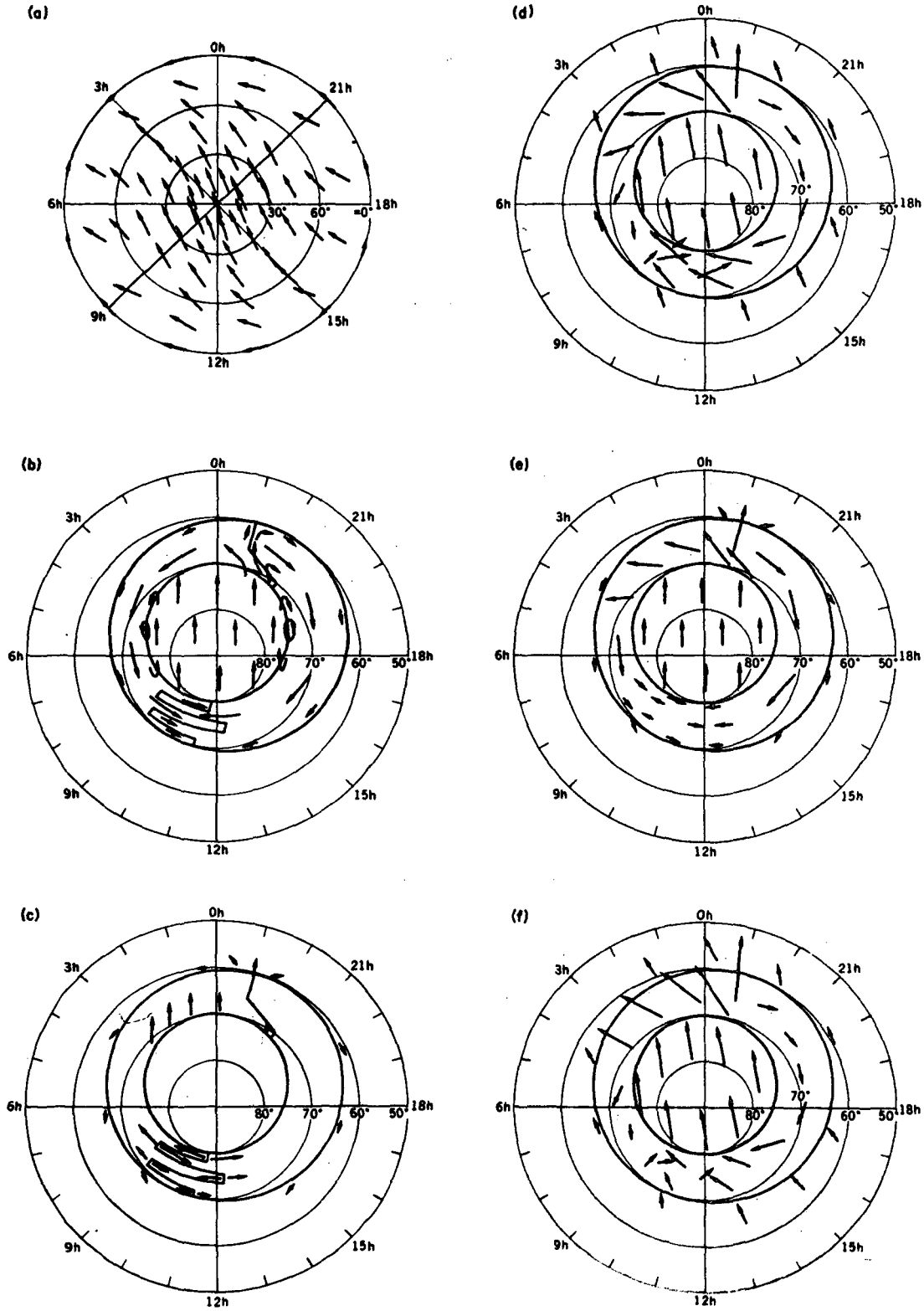
(a)
0h
3h
21h
6h
18h
9h
15h
12h
30°
60°
=0°
(d)
0h
3h
21h
6h
18h
9h
15h
12h
70°
80°
60°
50°
(b)
0h
3h
21h
6h
18h
9h
15h
12h
80°
70°
60°
50°
(e)
0h
3h
21h
6h
18h
9h
15h
12h
80°
70°
60°
50°
(c)
0h
3h
21h
6h
18h
9h
15h
12h
80°
70°
60°
50°
(f)
0h
3h
21h
6h
18h
9h
15h
12h
70°
80°
60°
50°

Figure 9